

Energy and spectral enhancement of femtosecond supercontinuum in a noble gas using a weak seed

Trenton R. Ensley,¹ Dmitry A. Fishman,¹ Scott Webster,¹ Lazaro A. Padilha,^{1,2}
David J. Hagan,¹ and Eric W. Van Stryland^{1,*}

¹College of Optics & Photonics: CREOL & FPCE, University of Central Florida, 4000 Central Florida Blvd., Orlando, Florida 32816-2700, USA

²Currently with Los Alamos National Laboratory, P.O. Box 1663, Los Alamos, New Mexico 87545, USA
ewvs@creol.ucf.edu

Abstract: We experimentally demonstrate that the use of a weak seed pulse of energy less than 0.4% of the pump results in a spectral energy enhancement that spans over 2 octaves and a total energy enhancement of more than 3 times for supercontinua generated by millijoule level femtosecond pulses in Krypton gas. Strong four-wave mixing of the pump-seed pulse interacting in the gas is observed. The spectral irradiance generated from the seeding process is sufficiently high to use white-light continuum as an alternative to conventional tunable sources of radiation for applications such as nonlinear optical spectroscopy.

©2011 Optical Society of America

OCIS codes: (190.4380) Nonlinear optics, four-wave mixing; (190.4975) Parametric processes; (320.6629) Supercontinuum generation; (320.7110) Ultrafast nonlinear optics.

References and links

1. R. R. Alfano, and S. L. Shapiro, "Observation of self-phase modulation and small-scale filaments in crystals and glasses," *Phys. Rev. Lett.* **24**(11), 592–594 (1970).
2. P. B. Corkum, C. Rolland, and T. Srinivasan-Rao, "Supercontinuum generation in gases," *Phys. Rev. Lett.* **57**(18), 2268–2271 (1986).
3. A. Brodeur, and S. L. Chin, "Band-gap dependence of the ultrafast white-light continuum," *Phys. Rev. Lett.* **80**(20), 4406–4409 (1998).
4. M. Kolesik, G. Katona, J. V. Moloney, and E. M. Wright, "Physical factors limiting the spectral extent and band gap dependence of supercontinuum generation," *Phys. Rev. Lett.* **91**(4), 043905 (2003).
5. P. B. Corkum, and C. Rolland, "Femtosecond continua produced in gases," *IEEE J. Quantum Electron.* **25**(12), 2634–2639 (1989).
6. G. Yang, and Y. R. Shen, "Spectral broadening of ultrashort pulses in a nonlinear medium," *Opt. Lett.* **9**(11), 510–512 (1984).
7. Y. Kamali, J.-F. Daigle, F. Théberge, M. Châteauneuf, A. Azarm, Y. Chen, C. Marceau, S. C. Lessard, F. Lessard, G. Roy, J. Dubois, and S. L. Chin, "Remote sensing of trace methane using mobile femtosecond laser system of T&T Lab," *Opt. Commun.* **282**(10), 2062–2065 (2009).
8. A. Couairon, H. Chakraborty, and M. B. Gaarde, "From single-cycle self-compressed filaments to isolated attosecond pulses in noble gases," *Phys. Rev. A* **77**(5), 053814 (2008).
9. M. Sheik-Bahae, A. A. Said, T. H. Wei, D. J. Hagan, and E. W. Van Stryland, "Sensitive measurement of optical nonlinearities using a single beam," *IEEE J. Quantum Electron.* **26**(4), 760–769 (1990).
10. M. Sheik-Bahae, A. A. Said, T. H. Wei, D. J. Hagan, and E. W. Van Stryland, "Special 30th anniversary feature: sensitive measurement of optical nonlinearities using a single beam," *IEEE LEOS Newsletter* **21**, 17–35 (2007).
11. M. Balu, J. Hales, D. J. Hagan, and E. W. Van Stryland, "White-light continuum Z-scan technique for nonlinear materials characterization," *Opt. Express* **12**(16), 3820–3826 (2004).
12. M. Balu, L. A. Padilha, D. J. Hagan, E. W. Van Stryland, S. Yao, K. Belfield, S. Zheng, S. Barlow, and S. Marder, "Broadband Z-Scan characterization using a high-spectral-irradiance, high-quality supercontinuum," *J. Opt. Soc. Am. B* **25**(2), 159–165 (2008).
13. M. Balu, L. A. Padilha, D. J. Hagan, E. W. Van Stryland, S. Yao, K. Belfield, S. Zheng, S. Barlow, and S. Marder, "Broadband Z-Scan characterization using a high-spectral-irradiance, high-quality supercontinuum: erratum," *J. Opt. Soc. Am. B* **26**(8), 1663 (2009).
14. J. Kasparian, R. Sauerbrey, D. Mondelain, S. Niedermeier, J. Yu, J.-P. Wolf, Y.-B. André, M. Franco, B. Prade, S. Tzortzikis, A. Mysyrowicz, M. Rodriguez, H. Wille, and L. Wöste, "Infrared extension of the super

- continuum generated by femtosecond terawatt laser pulses propagating in the atmosphere,” Opt. Lett. **25**(18), 1397–1399 (2000).
15. D. R. Solli, C. Ropers, and B. Jalali, “Active control of rogue waves for stimulated supercontinuum generation,” Phys. Rev. Lett. **101**(23), 233902 (2008).
 16. J. H. Kim, M. K. Chen, C.-E. Yang, J. Lee, K. Shi, Z. Liu, S. S. Yin, K. Reichard, P. Ruffin, E. Edwards, C. Brantley, and C. Luo, “Broadband supercontinuum generation covering UV to mid-IR region by using three pumping sources in single crystal sapphire fiber,” Opt. Express **16**(19), 14792–14800 (2008).
 17. C. Xiong, Z. Chen, and W. J. Wadsworth, “Dual-wavelength-pumped supercontinuum generation in an all-fiber device,” J. Lightwave Technol. **27**(11), 1638–1643 (2009).
 18. K. Wang, L. Qian, H. Luo, P. Yuan, and H. Zhu, “Ultrabroad supercontinuum generation by femtosecond dual-wavelength pumping in sapphire,” Opt. Express **14**(13), 6366–6371 (2006).
 19. K. Y. Kim, A. J. Taylor, J. H. Gownia, and G. Rodriguez, “Coherent control of terahertz supercontinuum generation in ultrafast laser-gas interactions,” Nat. Photonics **2**(10), 605–609 (2008).
 20. P. B. Petersen, and A. Tokmakoff, “Source for ultrafast continuum infrared and terahertz radiation,” Opt. Lett. **35**(12), 1962–1964 (2010).
 21. F. Théberge, N. Aközbek, W. Liu, A. Becker, and S. L. Chin, “Tunable ultrashort laser pulses generated through filamentation in gases,” Phys. Rev. Lett. **97**(2), 023904 (2006).
 22. I. V. Fedotov, A. B. Fedotov, P. A. Zhokhov, A. A. Lanin, A. D. Savvin, and A. M. Zheltikov, “Parametric transformation and spectral shaping of supercontinuum by high-intensity femtosecond laser pulses,” JETP Lett. **88**(3), 157–159 (2008).
 23. I. V. Fedotov, P. A. Zhokhov, A. B. Fedotov, and A. M. Zheltikov, “Probing the ultrafast nonlinear-optical response of ionized atmospheric air by polarization-resolved four-wave mixing,” Phys. Rev. A **80**(1), 015802 (2009).
 24. C. S. Liu, V. B. Pathak, and V. K. Tripathi, “Cross-phase modulation between lasers in a tunnel ionizing gas,” Phys. Plasmas **16**(5), 053102 (2009).
 25. A. S. Joshi, P. A. Naik, S. Barnwal, Y. B. S. R. Prasad, and P. D. Gupta, “A novel technique for measurement of self-generated magnetic fields and the plasma density in laser produced plasmas from the Faraday rotation using two color probes,” Opt. Commun. **283**(23), 4713–4716 (2010).
-

1. Introduction

White-light continuum (WLC) generation, often referred to as supercontinuum (SC) generation, has encouraged a great deal of research interest since the first observation of spectral broadening in condensed media [1] and ultimately in gases [2]. The physics behind these highly nonlinear processes has been studied extensively [3–6] and is still being investigated. WLC can, in principle, be utilized in a variety of applications such as remote sensing [7] and single-cycle pulse generation [8]. Of specific interest to us, WLC can be used for nonlinear spectroscopy, where the high spectral irradiance, ultra-broadband source of radiation confined in a single beam can replace conventional tunable sources of radiation such as optical parametric generators/amplifiers (OPGs/OPAs). It has been shown that the analysis of nonlinear materials by the conventional Z-Scan technique [9,10] using a broadband single-beam WLC generated in water [11] results in a more rapid characterization of their nonlinear optical properties. This rapid characterization technique has been extended to the use of WLC generated in a noble gas which yields larger energy output and the ability to characterize materials with moderate two-photon absorption cross sections and nonlinear refractive indices between 400 - 800 nm [12,13]. Although spectral expansion of the WLC to the mid-IR (4.5 μm) has been demonstrated using long focal length geometries [14], the inability to generate high spectral irradiance, broadband WLC sources in practical laboratory environments has limited the ability to use single beam sources of radiation as an alternative to OPGs/OPAs for rapid nonlinear optical characterization.

Spectral extension of the WLC by introducing seed pulses has been demonstrated in various condensed media [15–18]. The generation of single frequency, high energy radiation in the terahertz regime [19,20] and in the visible [21–23] by pump-seed pulse interactions in gases has also been reported. Since WLC generated in gases is not limited by the same energy restrictions of optical damage thresholds as condensed media, it is advantageous to use gas for high energy WLC generation.

In this work we present experimental evidence of large energy enhancement and spectral broadening of a single filament, WLC source of radiation by using a weak ($\sim\mu\text{J}$) fs seed pulse

to stimulate the nonlinearity generated from an intense (~mJ) fs pump beam. For different seed wavelengths, we observe strong Stokes and anti-Stokes broadening with spectral energy seen as part of the filament. We attribute these findings of energy and spectral enhancement in part to the strong four-wave mixing (FWM) interaction between pump and seed pulses in the filament and, possibly, to higher order cascaded nonlinearities.

2. Experimental setup

The experimental configuration is presented in Fig. 1. A Ti:Sapphire laser system (Clark-MXR, CPA 2010) producing ~1.4 mJ, ~150 fs (FWHM), 780 nm pulses at a 1 kHz repetition rate is used in our WLC studies. The output of the laser system is divided into two pulses by a beam splitter. The pump pulse (~0.4 – 0.6 mJ) is temporally delayed on an optical delay line and weakly focused into a 1.25 m chamber filled with krypton gas (40 psi) by a 1.5 m plano-convex lens. The energies used to generate a stable, single-filament, unseeded WLC resulted in peak irradiances, I , of $\sim 10^{12}$ W/cm². A 780 nm notch filter was used to block the pump from the resultant WLC at the output of the gas chamber.

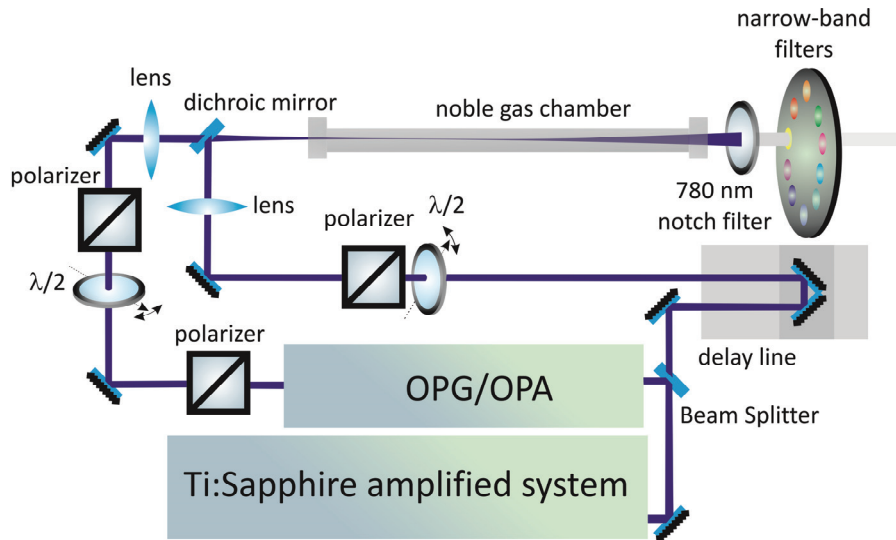


Fig. 1. Experimental configuration of seeded WLC.

The seed pulses were generated by pumping an OPG/OPA (TOPAS-800, Light Conversion, Ltd.) with ~0.4 mJ of the laser output. The wavelengths of the seed pulses ranged from 500 nm to 1300 nm. The seed pulses were focused by a 0.75 m plano-convex lens placed before the dichroic mirror and overlapped spatially and temporally with the pump. The combination of half-wave plates and polarizers were used to attenuate both the energies of the pump and seed pulses.

The WLC was spectrally analyzed by the use of a set of narrow band-pass interference filters ($\pm 4 - 8$ nm) at 40 - 50 nm increments. In all experiments the seed pulse energy did not exceed 1 μ J to ensure that the irradiance of the seed ($\sim 10^9$ W/cm²) was much less than that of the pump. Such low irradiances for the seed pulses are insufficient to induce filamentation from the seed alone.

3. Results and discussion

The typical spectra of the seeded and unseeded WLC are shown in Figs. 2(a, b) for a seed pulse energy of 1 μ J and pump pulse energy of ~0.4 mJ. The presence of the seed pulse results in a dramatic enhancement of the spectral irradiance. Without the seed pulse, the

typical WLC spectrum has an integrated energy of ~ 1250 nJ (area under the black curve of Fig. 2a).

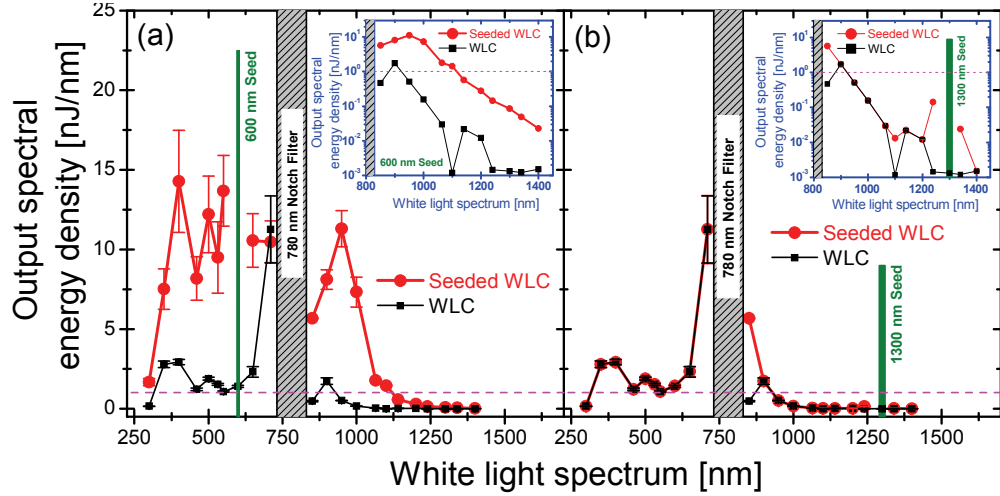


Fig. 2. Comparison of spectral output energy density of unseeded WLC (closed black squares) with seeded WLC (closed red circles) using (a) 600 nm seed and (b) 1300 nm seed of energy 1 μ J and pump energy of ~ 0.4 mJ. The dark green vertical line in (a) represents the 600 nm seed bandwidth and in (b) the 1300 nm seed bandwidth. The magenta horizontal dotted line denotes the typical energy density necessary to perform nonlinear optical characterizations using methods such as the WLC Z-Scan. The vertical shaded area in both figures represents wavelengths cut off by the 780 nm notch filter. The inset of (a) plotted on a log scale shows the spectral extension of the WLC on the Stokes side of the pump frequency, and the inset of (b) plotted on a log scale shows modest enhancement and broadening around the 1300 nm seed wavelength.

The stimulation by weak seed pulses of wavelengths within the unseeded WLC results in an increase of the total integrated energy to ~ 5800 nJ (area under the red curve of Fig. 2a), i.e. more than 360% enhancement for this seeding wavelength. In the case of WLC Z-Scan, the unseeded WLC typically yields a usable wavelength range (denoted by a spectral energy density of ≥ 1 nJ / nm) of 400 nm – 800 nm for nonlinear optical characterization. The introduction of the weak seed pulse extends the usable range from 300 nm to > 1100 nm (see Fig. 2a, inset). At 1000 ± 7 nm (the typical cutoff of our unseeded WLC), we measure the largest enhancement utilizing a 650 nm seed resulting in 14.2 ± 0.6 nJ / nm versus ~ 0.17 nJ / nm, i.e. an 83x increase. The enhancement at this particular wavelength can be attributed to FWM where $\lambda^{-1}_{\text{FWM}} = 2\lambda^{-1}_{\text{Pump}} - \lambda^{-1}_{\text{Seed}}$. However, we also see significant enhancement at wavelengths not directly associated with FWM. For instance, the 600 nm seeded WLC yields nearly 10 nJ / nm output at 532 ± 4 nm compared to 1.5 nJ / nm output for an unseeded WLC, resulting in more than 6x enhancement with a seed pulse energy $\sim 0.3\%$ that of the 780 nm pump. For seed wavelengths outside of the unseeded WLC spectrum, only modest enhancement and spectral broadening around the seed wavelengths are observed as shown in Fig. 2b.

Figure 3 provides the experimental map of the WLC spectrum seeded with different wavelengths with the same seed pulse energy (1 μ J). As was stated previously, the largest enhancement and spectral broadening occurs for seeding in the visible range. Seed wavelengths slightly above and below that of the pump could not be utilized due to the limitations of the energy output of the OPA and/or the broad bandwidth of our highly reflective dichroic mirror cutting off wavelengths close to that of the pump. Therefore, no information could be obtained from the “experimental gap” region in Figs. 3 and 4 (described

below). Additionally, the WLC may extend further into the UV region below 300 nm but due to the spectral notch filter's cutoff in the UV this could not be determined.

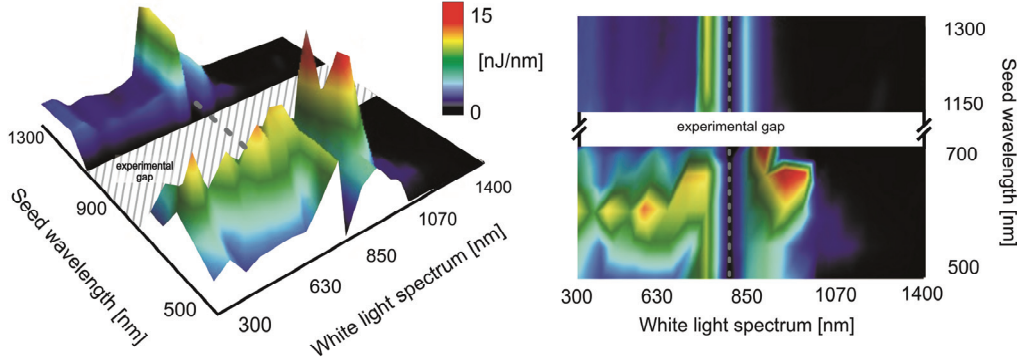


Fig. 3. Spectral energy density map of the WLC spectra at different seed pulse wavelengths. The figure on the right shows the top view of the spectrum and the figure on the left shows the side view. The area labeled “experimental gap” represents seed wavelengths that could not be utilized due to either the broad reflective bandwidth of the dichroic mirror or insufficient energy output of the OPA. The vertical gray dotted line represents unmeasured spectral regions that were inaccessible due to the cutoff of the 780 nm notch filter.

We measured the dependence of the WLC enhancement on the time delay between pump and seed pulses as shown in Fig. 4. The output light was collected onto either a silicon or germanium photodiode covering a range from ~ 200 nm to ~ 1800 nm, respectively. In Fig. 4a the irradiance at 532 ± 4 nm is shown for seed wavelengths of 600 nm and 1300 nm. The enhancement for each seeded wavelength occurs at the zero delay between the seed and pump pulse, which was determined by sum frequency generation on a 1 mm thick Type-I BBO crystal.

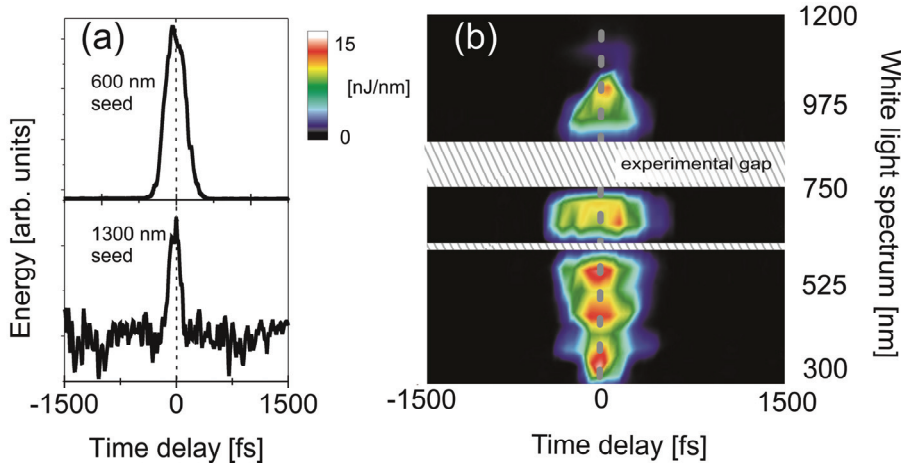


Fig. 4. (a) Energy within an 8 nm FWHM bandwidth centered at 532 nm using seed pulses at 600 nm and 1300 nm versus time delay between the pump and seed pulse, and (b) differential spectral energy density map of WLC spectrum using a fixed 600 nm seed and recording the temporal behavior of the white-light spectrum at different time delays between pump and seed pulses. The large shaded area, labeled “experimental gap”, in (b) represents spectral regions that could not be measured due to the cutoff of the 780 nm notch filter. The small shaded area represents the 600 nm seed bandwidth.

For fixed seed wavelengths, the overall behavior of the spectral enhancement has similar dynamics as shown in Fig. 4b. The data presented in Fig. 4b is the difference between when the pump and seed pulses are temporally overlapped and not, i.e. the enhancement. The broadening is seen to follow closely the temporal width of the pump beam. Moreover, the peak of the spectral enhancement occurs near zero delay which implies that the stimulated generation and energy enhancement occur near the initiation of filamentation for all wavelengths.

Table 1. Output WLC energy density for different seed wavelengths. The unseeded output WLC energy density is given in parenthesis for comparison. In the case of “Total WLC Energy”, the seed pulse energy ($\sim 1 \mu\text{J}$) transmitted in the absence of the pump ($\sim 0.4 \text{ mJ}$) was subtracted from the total reading.

Seed wavelength (nm)	WLC Energy Density @ 532 nm (nJ / nm)	WLC Energy Density @ 1000 nm (nJ / nm)	Total WLC Energy (μJ)
500	3.6 ± 1.2 (1.5)	3.9 ± 0.4 (0.17)	3.1 (1.2)
550	7.5 ± 2.1 (1.5)	2.3 ± 0.1 (0.17)	2.8 (1.2)
600	9.5 ± 2.2 (1.5)	7.2 ± 0.9 (0.17)	3.7 (1.2)
650	6.7 ± 1.2 (1.5)	14.2 ± 0.6 (0.17)	3.8 (1.2)
710	4.0 ± 0.7 (1.5)	1.1 ± 0.02 (0.17)	1.9 (1.2)
1150	2.5 ± 0.8 (1.5)	0.9 ± 0.3 (0.17)	1.3 (1.2)
1200	1.6 ± 0.2 (1.5)	0.3 ± 0.01 (0.17)	1.21 (1.2)
1240	1.5 ± 0.1 (1.5)	0.2 ± 0.01 (0.17)	1.3 (1.2)
1300	1.5 ± 0.1 (1.5)	0.17 ± 0.01 (0.17)	1.21 (1.2)

Table 1 shows the WLC energy densities at $532 \pm 4 \text{ nm}$ and $1000 \pm 7 \text{ nm}$ with and without the seed (500 nm to 1300 nm). For example, a 500 nm seed yields an energy density at 1000 nm of 3.9 nJ / nm compared to 0.17 nJ / nm unseeded, i.e. an enhancement of 23. The largest enhancement at 532 nm and 1000 nm occurs with seed inputs in the visible spectral range with a peak near 600 nm at 532 nm and 650 nm for 1000 nm. Also shown (last column) is the overall enhancement of the total WLC energy with different seeds.

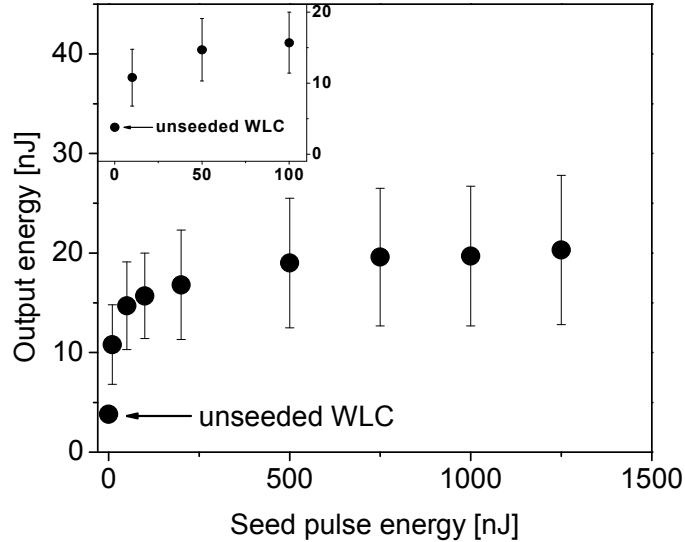


Fig. 5. Output energy at $532 \pm 4 \text{ nm}$ as a function of seed pulse energy at 600 nm. The inset shows the first four data points of Fig. 5. Enhancement was observed with a seed pulse energy less than 10 nJ. An aperture was used to observe the energy confined in the single filament WLC as opposed to any possible scattered radiation from the seed-plasma interaction. Note that the lowest energy data point in both graphs corresponds to the unseeded WLC.

The total seeded WLC output energy is ~ 3 times greater than that of the unseeded WLC for the case of visible seeds reaching a maximum of ~ 3.2 for a seed of 650 nm. Since the seed pulses were kept at $\sim 1 \mu\text{J}$, this implies that the seeding process not only increases the energy around the input but stimulates the transfer of energy from the pump into the WLC. Figure 5 shows the enhancement of the WLC output at 532 ± 4 nm as a function of the seed pulse energy. The enhancement is initiated at extremely small energies ($\sim \text{nJ}$) and saturates above $\sim 100 \text{ nJ}$.

While FWM between the pump and visible seed ($2\omega_p - \omega_s$) may help to explain the extension of the WLC to longer wavelengths in the near IR, it does not explain the remarkable enhancement observed across the visible. Calculations like those of Liu et al. [24] simulate the effects of a strong pump pulse on a seed beam, which do not account for the dramatic changes that we observe on the pump. For example, the authors of Ref [24]. show that the ionization front induced by the pump causes a frequency blue-shift of the *seed* pulse when its maximum irradiance lies at the same position as the ionization front. This may be among the effects involved in our experiments, but processes with gain to transfer energy from the pump to other wavelengths must be present.

4. Conclusions

The spectral energy of the WLC as well as the total WLC energy is enhanced by more than 3 times by using extraordinarily weak seed pulses in the visible regime having energies less than 0.4% that of the pump. These results have significant implications for experiments aimed at probing the plasma generated from a pump source [25]. Pump-probe experiments rely on the probe not significantly affecting the pump or signal which is obviously violated in our experiments. A complete physical explanation of these phenomena awaits simulation; however, it is likely that strong four-wave mixing between the pump and seed pulses in the filament along with higher order cascaded nonlinearities are the causes. These findings lay the groundwork for creating a high spectral irradiance, ultrabroad WLC source that may be used as an alternative to conventional tunable sources of radiation for applications such as nonlinear optical spectroscopy.

Acknowledgements

The authors thank Dr. B.Ya. Zeldovich for useful discussions. This work is supported in part by the U. S. Army Research Office under contract/grant 50372-CH-MUR, the Air Force Office of Sponsored Research MURI AFOSR grant FA9550-06-1-0337, the DARPA ZOE program grant W31R4Q-09-1-0012, and the Israel Ministry of Defense contract 993/54250-01.